Signaling from germ cells mediated by the *rhomboid* homolog *stet* organizes encapsulation by somatic support cells

Cordula Schulz, Cricket G. Wood*, D. Leanne Jones, Salli I. Tazuke and Margaret T. Fuller[†]

Departments of Developmental Biology and Genetics, Stanford University School of Medicine, Stanford, CA 94305-5329, USA
*Present address: Neuroscience Research Institute, University of California Santa Barbara, Santa Barbara, CA 93106, USA
[†]Author for correspondence (e-mail address: fuller@cmgm.stanford.edu)

SUMMARY

Germ cells normally differentiate in the context of encapsulating somatic cells. However, the mechanisms that set up the special relationship between germ cells and somatic support cells and the signals that mediate the crucial communications between the two cell types are poorly understood. We show that interactions between germ cells and somatic support cells in *Drosophila* depend on wild-type function of the *stet* gene. In males, *stet* acts in germ cells to allow their encapsulation by somatic cyst cells and is required for germ cell differentiation. In females, *stet* function allows inner sheath cells to enclose early germ cells correctly at the tip of the germarium. *stet* encodes a homolog of *rhomboid*, a component of the *epidermal growth factor receptor* signaling pathway involved in ligand activation in the signaling cell. The *stet* mutant phenotype suggests that *stet* facilitates signaling from germ cells to the *epidermal growth factor receptor* on somatic cells, resulting in the encapsulation of germ cells by somatic support cells. The micro-environment provided by the surrounding somatic cells may, in turn, regulate differentiation of the germ cells they enclose.

Key words: Somatic niche, Stem cells, Gametogenesis, Signaling, Rhomboid homolog, *Drosophila*

INTRODUCTION

Germ cells normally differentiate while in intimate contact with somatic support cells. In mammals, differentiating male germ cells are enclosed in somatically derived Sertoli cells (Desjardins and Ewing, 1993) and oocytes are surrounded by somatic granulosa cells (Erickson, 1986; Hsuesh and Schomberg, 1993). In both cases, interactions between germ cells and surrounding somatic cells play important roles in gametogenesis (Marziali et al., 1993; Bitgood et al., 1996; Pesce et al., 1997; Ojeda et al., 2000; Matzug, 2000). Similarly, in *Caenorhabditis elegans,* early germ cells are closely associated with the somatic distal tip cell, which provides crucial signals that govern germ cell proliferation versus differentiation (Kimble and White, 1981; Berry et al., 1997). At subsequent stages, *C. elegans* germ cells interact with somatic sheath and spermathecal cells (Church et al., 1995; McCarter et al., 1997; Hall et al., 1999). In insects as well, germ cells are closely associated with somatic cells (King, 1970; Hardy et al., 1979; Bünning, 1994), which play key regulatory roles in germ cell fate (reviewed by Kiger and Fuller, 2001; Xie and Spradling, 2001).

In *Drosophila* males, germline stem cells lie at the apical tip of the testis, in intimate contact with somatic hub and cyst progenitor cells. Upon stem cell division, the daughter cell displaced away from the hub becomes encapsulated by two somatic cyst cells and initiates differentiation (Hardy et al., 1979). The surrounding somatic cyst cells play an important

role in the initiation of germ cell differentiation (Kiger et al., 2000; Tran et al., 2000), and later in the transition from mitosis to meiosis (Gönczy et al., 1997; Matunis et al., 1997). In *Drosophila* females, somatic cells at the apical tip of the germarium form a specialized niche in which germline stem cells are maintained through signaling from the soma (Xie and Spradling, 1998; King and Lin, 1999; Xie and Spradling, 2000). After mitotic amplification, clusters of 16 interconnected female germ cells become surrounded by follicle cells, which form an epithelial sheath around each developing egg chamber. Interactions between germ cells and follicle cells regulate such critical events as egg chamber formation and determination of the polarity of the developing oocyte (reviewed by Ray and Schüpbach, 1996; Morgan and Mahowald, 1996).

Signaling via the *epidermal growth factor receptor* (*Egfr*) mediates many cell-cell interactions where one cell influences the proliferation or differentiation of a closely apposed partner (Schweitzer and Shilo, 1997; Freeman, 1998). Despite the exquisitely localized and temporally specific requirements for *Egfr* activation in normal development documented in *Drosophila*, the *Egfr* and its major ligand *spitz* (*spi*) are widely expressed (Lev et al., 1985; Kammermayer and Wadsworth, 1987; Rutledge et al., 1992). Spatial and temporal control of *Egfr* pathway activation appear to be achieved at the level of ligand activation. *spi* is synthesized as a transmembrane protein. Proteolytic cleavage of *spi* by the transmembrane protein rh*omboid* (*rho*) within the Golgi apparatus of the signal

sending cell produces a potent diffusible ligand (Rutledge et al., 1992; Schweitzer et al., 1995; Golembo et al., 1996; Lee et al., 2001; Urban et al., 2001). Expression of *rho* is spatially and temporally controlled, providing developmental specificity to activation of the *Egfr* pathway (Bier et al., 1990)

In *Drosophila* oogenesis, germ cells signal via the germline *Egfr* ligand *gurken* (*grk*) to specify the correct behavior of follicle cells in encapsulating each individual cluster of 16 germ cells (Goode et al., 1992), and later to pattern the follicle cell layer (Schüpbach, 1987; Gonzales-Reyes et al., 1995). So far it has been unclear how *Egfr* is activated during oogenesis. Germline clones mutant for *rho* produced wild-type eggs, suggesting that *rho* is not required in germ cells. Instead, *rho* is expressed in follicle cells depending on *Egfr* activation (Ruohola-Baker et al., 1993), most likely to spread and amplify the initial signaling event (Wasserman and Freeman, 1998).

We show that *stet*, a homolog of *rho*, plays a crucial role in signaling from germ cells to somatic cells. Wild-type function of *stet* is required for encapsulation of germline stem cells and their progeny by somatic support cells and germ cell differentiation in both *Drosophila* males and females. Clonal analysis and rescue experiments in testes have demonstrated that *stet* function is required in germ cells. The conserved protease motif in the Stet protein (Urban et al., 2001) and its subcellular localization (Ghiglione et al., 2002) suggest that *stet* functions through the same biochemical mechanism as *rho*. In support of this, expression of *rho* in germ cells rescued the *stet* mutant testes phenotype. We propose that *stet* activates signaling from germ cells to the *Egfr* on somatic support cells to set up the crucial associations between germ cells and soma that are required for normal gamete differentiation.

MATERIAL AND METHODS

Fly strains

Flies were raised on standard cornmeal molasses agar medium at 25°C. The original allele *stet^{871}* was identified in an EMS screen for male sterility by J. Hackstein. Seven *stet* alleles (*stet$^{1, 2, 3, 8A, 8B, 8F, 9}$*) were isolated on a *red, ebony* chromosome in a screen in our laboratory for EMS induced mutations that failed to complement a chromosome carrying the *stet^{871}* allele. Six additional *stet* alleles (*stet$^{Z3-0369, z3-4806, z3-3671, z3-0919, z3-3835, z3-2244}$*) were identified as male sterile mutations by B. Wakimoto and D. Lindsley in a collection of 12000 EMS-induced viable lines generated in the laboratory of C. Zucker. We identified these Zucker lines as carrying *stet* alleles by failure to complement the *stet^{871}* allele. All other *Drosophila* mutants and balancer chromosomes are as described elsewhere (Lindsley and Zimm, 1992).

stet mapping

The *stet^{871}* mutation was mapped by recombination between *roughoid* (*ru*) and *hairy* to 1.4 map units proximal to *ru*. *stet* was localized to polytene interval 62A1 with the following deficiencies generated in our laboratory: *stet* was uncovered by *Df(3L)29b* (61C;62A5) and *Df(3L)PX62* (62A1), but not by *Df(3L)PX49-15* (62A1;A8). The generation of deficiencies and their breakpoints are described elsewhere (Schulz et al., 2002). The *stet* mutant phenotype was analyzed in flies trans-heterozygous for loss-of-function alleles *stet^{871}*, *stet^{2}* and *stet$^{z3-3671}$* over *Df(3L)PX62*. *stet^{871}*, *stet^{2}* and *stet$^{z3-3671}$* displayed the same phenotype trans-heterozygous to each other as over *DF(3L)PX62*. However, *stet^{871}* and *stet$^{z3-3671}$* carried additional mutations on their chromosomes, giving rise to stronger

phenotypes in ovaries when homozygous. Unless otherwise stated, images of *stet* mutant gonads shown were from *stet^{871}/Df(3L)PX62* animals.

X-gal staining, immunofluorescense and histochemistry, GAL4/UAS expression studies

Ovaries and larval testes were stained for immunofluorescence, histochemistry, or β-galactosidase activity following standard protocols (Ashburner, 1989). Testes used for anti-Map-kinase immunohistochemistry were dissected in testes buffer with phosphatase inhibitors (10 mM Tris-HCl, pH 6.8, 180 mM KCl, 50 mM NaF, 10 mM NaVO$_4$ and 10 mM β-glycerophosphate) before the staining procedure. Immunofluorescence experiments on squashed testes were performed as described previously (Hime et al., 1996). The hybridoma/monoclonal antibodies mouse anti-α-spectrin (1:5) (developed by D. Branton and R. Dubreuil), mouse anti-fasciclin III (1:10) (developed by C. Goodman) and mouse anti-Sxl (1:200) (developed by P. Schedl) were obtained from the Developmental Studies Hybridoma Bank developed under the auspices of the NICHD and maintained by The University of Iowa, Department of Biological Sciences, Iowa City, IA 52242. The monoclonal mouse anti-Map-kinase antibody (Sigma) was used at 1:200, polyclonal rabbit anti-phosphorylated Histone-H3 antibody (Upstate Biotechnology, NY) was used at 1:100. Secondary antibodies (Jackson Immuno Research Laboratories) were used at 1:200. DAPI (Sigma) was used at 1 μg/ml. Counts of cell types were performed by scoring 20 to 50 testes or ovarioles of wild-type and *stet* mutant animals. Expression of UAS-constructs under control of the GAL-4 activator proteins (Phelps and Brand, 1998) were temporally controlled by growing flies at 18°C and shifting them to 29°C as larvae, pupae or adults.

In situ hybridization

Whole-mount in situ hybridization was performed as described by Tautz and Pfeifle (Tautz and Pfeifle, 1989), with modifications for RNA probes described by Klingler and Gergen (Klingler and Gergen, 1993). Ribonucleotide probes were generated from linearized plasmid using the Roche Molecular Biochemicals (Indianapolis) RNA-labeling kit.

Clonal analysis

The alleles *stet^{871}* and *stet$^{Z3-3671}$* were recombined onto FRT-80 chromosomes (FRT-80-stet). Males carrying the FRT-80-stet chromosome and control animals carrying the FRT-80 chromosome were crossed to females carrying the FLP recombinase gene under control of a heat-shock promoter and a FTR-80 chromosome marked with a nuclear targeted GFP (FRT-80-GFP). Progeny were heat-shocked during pupal stages or as adults for 2 hours in a 37°C waterbath. Testes from adult males were dissected 7 to 10 days after heat-shock. On average, one out of seven testes showed GFP-negative clones. Under these conditions, control animals often contained several clusters of GFP negative cells, while males carrying the FRT-80-*stet* chromosome usually contained only one cluster of GFP negative clones (nine out of 10 testes with clones scored).

Molecular cloning

All molecular techniques were performed using standard protocols (Sambrook et al., 1989). The genomic walk across cytological region 62A is described elsewhere (Schulz et al., 2002). The left molecular breakpoint of *Df(3L)PX62* mapped in cosmid 116G11, in the 5′ non-translated region of the rho gene. The right breakpoint of *Df(3L)PX62* mapped in cosmid 6814, 250 bp 5′ of the *Drosophila puromycin-sensitive aminopeptidase* gene translational start. 11 of the 12 potential transcription units in the 62A1 area were determined not to be *stet* by several approaches. Some of the transcription units were excluded because known mutant alleles complemented *stet* mutants. Others were excluded because genomic rescue constructs potentially containing the whole transcription units did not rescue the *stet* mutant
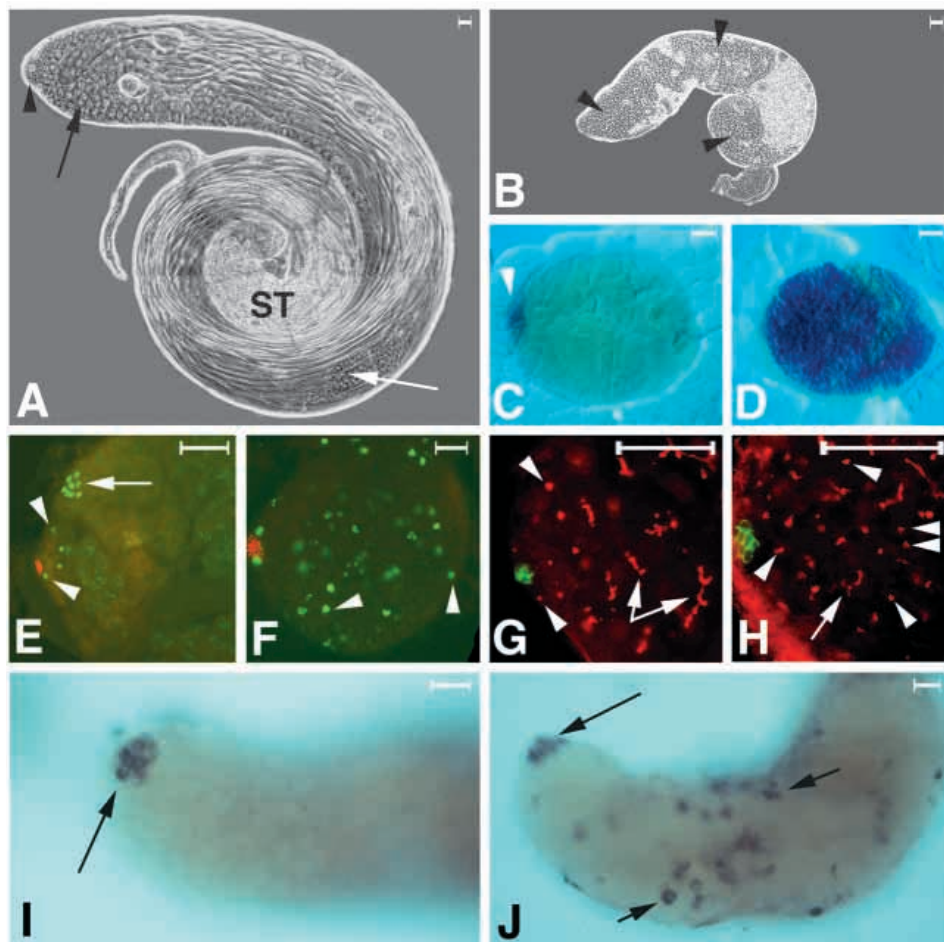
Fig. 1. Early germ cells accumulate in *stet* mutant testes. (A,C,E,G,I) Wild-type and (B,D,F,H,J) *stet* mutant testes, apical tips towards the left. Scale bars: 0.1 mm. (A,B) Phase-contrast images of adult (A) wild-type and (B) *stet* [871] mutant testes; small early germ cells (arrowheads) at the apical tip of wild-type testes and throughout *stet* mutant testes. Larger spermatocytes (black arrow) displaced away from the tip, differentiating round spermatids (white arrow) along the coil of the testis, bundles of elongated spermatids (ST), in wild type as indicated. (C,D) Third instar larval testes showing cells expressing the S3-46 marker (C) at the tip of wild-type testis (arrowhead) and (D) filling almost the entire *stet* mutant testis. (E,F) Third instar larval testes from (E) wild-type and (F) *stet* stained with anti-FasIII (red) and anti-phosphorylated Histone-H3 (green). Single anti-phosphorylated H3-positive cells are indicated by arrowheads. Dividing spermatogonia (arrow) are seen as clusters of eight anti-phosphorylated Histone-H3-positive cells in wild type. (G,H) Third instar larval testes stained with anti-FasIII (green) and anti-α-spectrin (red) of (G) wild-type and (H) *stet* with α-spectrin staining in spectrosomes (arrowheads) and in branched fusomes (arrows). Note slightly enlarged apical hub (green) in *stet* mutant testis compared with wild type. (I,J) In situ hybridization with *esg* mRNA in adult (G) wild-type and (H) *stet* mutant testes. Arrows indicate *esg*-positive cells at tip in wild type.

phenotype when introduced into flies by P-element-mediated transformation (Spradling, 1986). Finally, for those of the 11 transcription units expressed in testes, we did not detect lesions in the coding regions when sequencing several strong *stet* alleles. Molecular information about the 62A area, cDNA clones of transcripts in this interval, as well as information about their expression pattern, and several genomic rescue constructs are available from the authors on request.

RESULTS

stet function is required for male germ cell differentiation

Wild-type function of the *stet* locus is required for male germ cells to proceed through early stages of differentiation. Loss-of-function stet mutant males were viable but sterile. Adult *stet* mutant males had tiny testes filled with small cells (Fig. 1B, arrowheads) resembling cells normally found only at the tip of wild-type testis (Fig. 1A, arrowhead). Early male germ cells failed to differentiate and instead accumulated in third instar larval testes from loss-of-function *stet* animals, based on appearance in phase contrast and DIC microscopy, nuclear size in DAPI-stained preparations (data not shown) and expression of cell-type specific markers. In wild type, early germ cells

(stem cells, gonialblasts and spermatogonia) are located at the apical tip of the testis (Fig. 2A) and express the *lacZ* enhancer trap marker S3-46 (Fig. 1C, arrowhead). Spermatocytes are located more distally, fill most of the larval testis and do not express the S3-46 enhancer trap marker. Larval testes from *stet* mutant males were filled with cells expressing β-galactosidase from the S3-46 marker, suggesting that they were early germ cells (Fig. 1D).

In wild-type testes, mitotically active early germ cells were observed exclusively at the apical tip upon staining with anti-phosphorylated Histone-H3 antibody. Germline stem cells and gonialblasts divide as single cells (Fig. 1E, arrowheads), while spermatogonia divide in groups of two, four or eight cells (Fig. 1E, arrow). In *stet* mutants, many phosphorylated Histone-H3-positive cells were scattered throughout the testes, suggesting that the early germ cells accumulating in *stet* mutant testes remained mitotically active. Many anti-phosphorylated Histon-H3-positive cells were detected as single cells throughout *stet* mutant testes (Fig. 1F, arrowheads), indicating that cells with stem cell or gonialblast identity had been displaced away from the tip.

stet mutant testes appeared to contain a mixture of germ cells with stem cell, gonialblast and spermatogonial identities. In wild-type testes, α-spectrin is localized to a ball-shaped spectrosome in germline stem cells and gonialblasts and to the
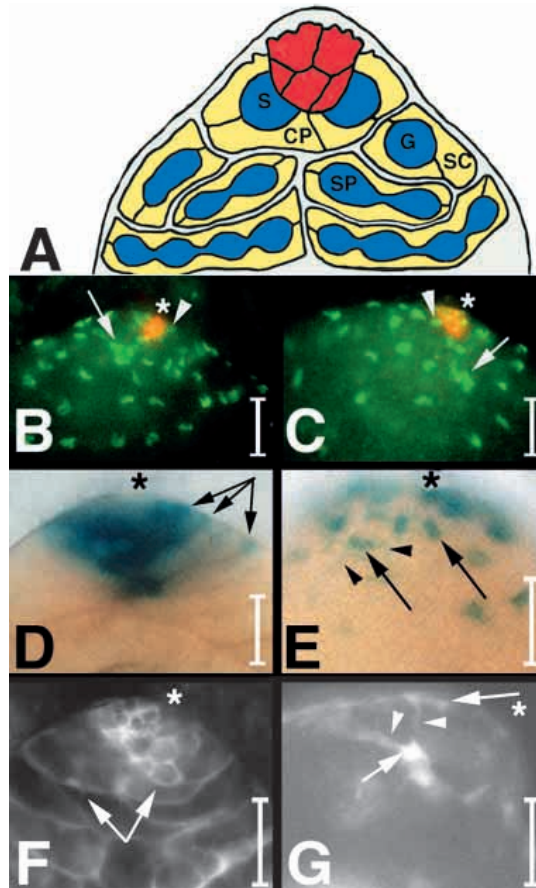
Fig. 2. Somatic cyst cells do not correctly surround germ cells in *stet* mutant testes. (A) Diagram of a cross-section through the apical tip of a wild-type testis. Germ cells in blue, somatic cyst cells in yellow. Germline stem cells (S) and cyst progenitor cells (CP) next to the apical somatic hub (red); gonialblast (G), spermatogonia (SP) and somatic cyst cells (SC), as indicated. (B-G) Testes from (B,D,F) wild type and (C,E,G) *stet* mutants. Asterisks indicate apical tips. Scale bars: 0.1 mm. (B,C) Third instar larval (B) wild-type and (C) *stet* mutant testis tip stained with anti-FasIII (red) to label the hub and anti-Tj (green) to label cyst progenitor nuclei next to the hub (arrowheads). Cyst cell nuclei are displaced away from the hub (arrows). (D,E) Third instar larval wild-type and *stet* mutant testis tip stained for β-galactosidase activity from the 17-en-40 marker. (D) Wild-type: cyst cells extend to surround the germ cells (arrows). (E) *stet*: β-galactosidase is detected in dots (arrows) and small cytoplasmic extensions (arrowheads). (F,G) Adult wild-type and *stet* mutant testis tip expressing UAS-GFP under control of the *ptc*-GAL4 activator. (F) Wild-type: GFP is detected in extensions (arrows) surrounding the germ cells. (G) *stet*: GFP is mostly detected in dots (arrows) and a few extensions (arrowheads).

branched fusome structure passing through the intercellular bridges between spermatogonia (Fig. 1G). In wild-type testes, 10 to 20 cells with a spectrosome dot could be detected at the apical tip. In *stet* mutant testes, we detected 20 to 40 cells with spectrosome dots (Fig. 1H, arrowheads) at the apical tip, and many cells with a spectrosome dot displaced away from the tip, suggesting an increased number of stem cells and/or gonialblasts. However, most of the small germ cells accumulating in *stet* mutant testes were interconnected by
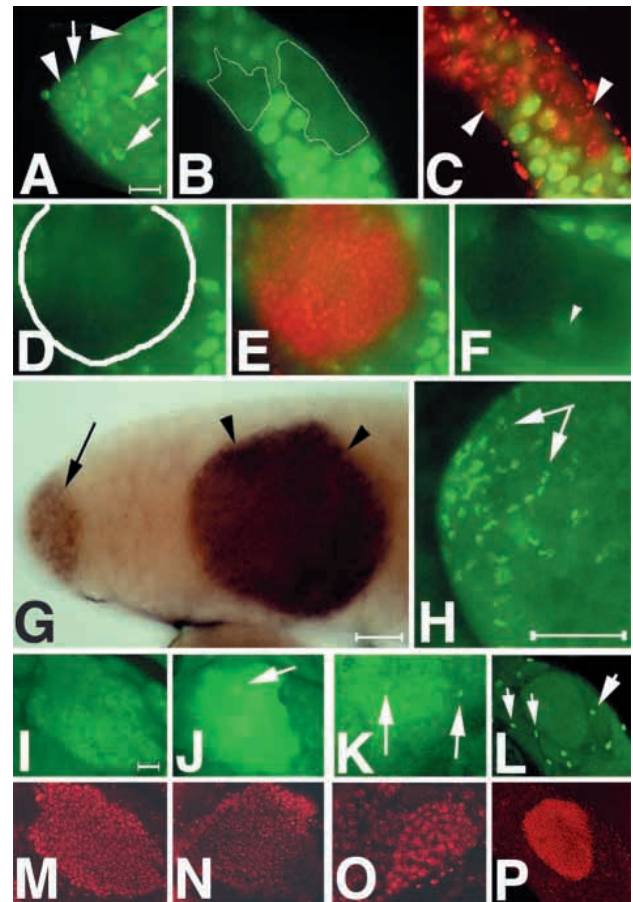
Fig. 3. Wild-type function of *stet* is required in the male germline. (A) Apical tip of a testis expressing nuclear ubiquitin-GFP. Nuclei of early germ cells at the apical tip and spermatocytes are seen as round GFP-signals (arrowheads), while nuclei of somatic cyst cells appear triangular (arrows). (B) Wild-type control clones (outlined) marked by lack of nuclear targeted GFP. Somatic cyst cell nuclei were detected associated with these clones out of focus in the image shown. (C) Same testes as in (B) double labeled for GFP and DAPI (red). GFP-negative cells in control clones differentiate normally and have large size DAPI-stained spermatocyte nuclei (arrowheads). (D) *stet* mutant germline clone (outlined) marked by lack of nuclear targeted GFP. (E) Same clone as in D double labeled for GFP and DAPI (red), GFP-negative cells contain small bright DAPI-stained nuclei. (F) *stet* mutant germline clone. No triangular GFP-positive nuclei were detected on top, under or beside the clone; dying cells in *stet* mutant testes autofluoresce (arrowhead). (G) Cells in a *stet* mutant clone (arrowheads) express *piwi*-RNA, a marker usually expressed only in early germ cells at the apical tip (arrow). (H-L) Immunofluorescence staining with anti-Tj. (H) Cyst cell nuclei (arrows) at the tip of a *stet*/+ testes. (I) Clone of *stet* mutant germ cells located further basally in the testes shown in H; *stet* mutant germ cells appear slightly brighter than the surrounding *stet*/+ spermatogonia because of background staining. No Tj-positive cyst cell nuclei were detected associated with the *stet* mutant germ cells. (J,K) Examples of *stet* mutant germ cell clones associated with (J) one and (K) two Tj-positive nuclei (arrows). (L) Cyst cell nuclei (arrows) stained for the late cyst cell marker Eya were associated with neighboring *stet*/+ spermatocytes, but not with the clone of *stet* mutant germ cells in the center of the image. (M-P) DAPI images of clones corresponding to images in I-L, respectively. Note the many small brightly stained nuclei. Scale bars: in A, 0.1 mm for A-F; in G, 0.1 mm; in H, 0.1 mm; in I, 0.1 mm for I-P.

Fig. 4. Defects in *stet* mutant ovarioles. DAPI staining of (A) wild-type and (B-D) *stet* mutant ovarioles in the same magnification, apical tips towards the left, germarium (g) at the apical tip. Scale bar: 0.1 mm. (A) Wild-type ovariole showing egg chambers at different developmental stages; nurse cells (nc) and oocyte (oc) as indicated, egg chambers contain 16 germ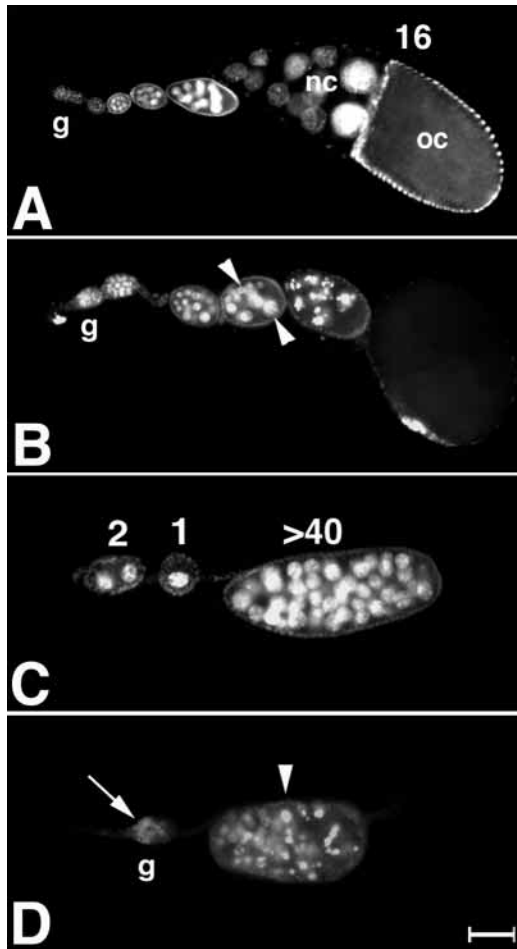 cells. (B) Ovariole from a young *stet* mutant female showing egg chambers at many stages. Note egg chambers with different sized nurse cell nuclei (arrowheads). (C) Egg chambers from a young *stet* mutant female showing abnormal numbers of germ cells, as indicated. (D) Ovariole from a 10-day-old *stet* mutant female showing germ cells at the apical tip (arrow) and degenerating egg chamber (arrowhead).

short, branched fusomes, suggesting spermatogonial identity (Fig. 1H, arrows).

Staining for *escargot* (*esg*) mRNA also suggested an increased number of cells with stem cell characteristics. In wild-type, *esg* mRNA was detected in the somatic hub cells and in the five to nine germline stem cells around the hub (Fig. 1I, arrow), but not in gonialblasts and spermatogonia. *stet* mutant testes had in average 40 *esg*-positive cells, ranging from the normal five to more than 100, with some at the apical tip and some displaced away from the apical tip (Fig. 1J, arrows).

Staining for somatic hub cell *lacZ* enhancer trap markers (254, S2-11) or the hub cell surface marker Fasciclin III (FasIII) revealed that somatic hub cells were present at the apical tips of *stet* third instar larval testes (Fig. 1F,H). However, the hub often appeared slightly enlarged and less tightly packed
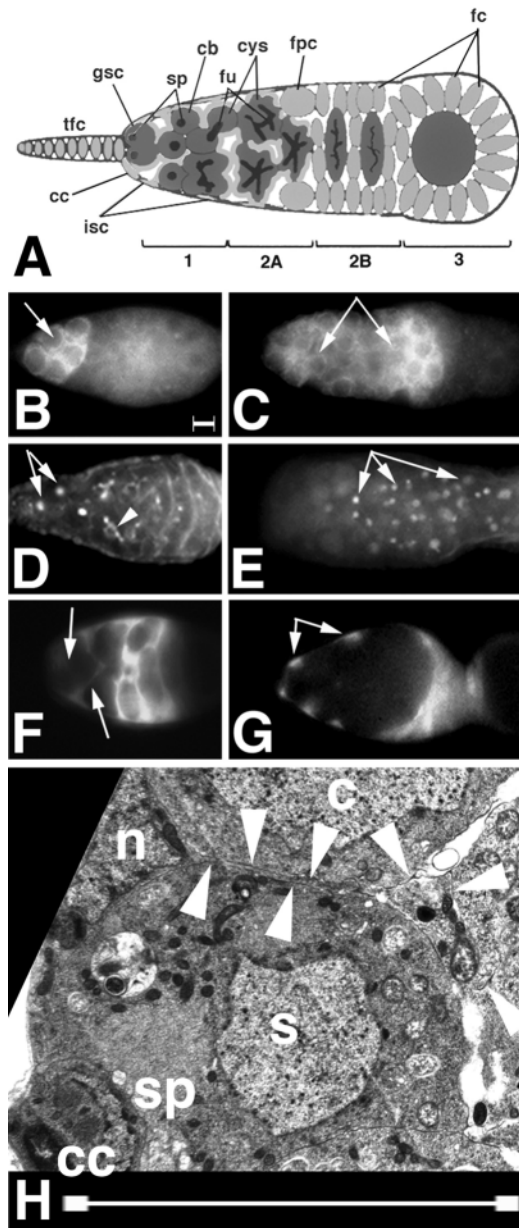
than in wild type (Fig. 1E,G), much as in agametic testes from sons of *oskar* mutant mothers (Gönczy et al., 1992).

In wild-type testes, somatic cyst progenitor cells act as stem cells for the cyst cell lineage (Gönczy and DiNardo, 1996) and lie next to the hub adjacent to germ line stem cells (Fig. 2A). The cyst progenitor cells produce somatic cyst cells, two of which encapsulate each gonialblast and its progeny throughout all subsequent stages of male germ cell differentiation. Somatic cyst cells and cyst progenitor cells were present in loss-of-function *stet* mutant testes based on the presence of *traffic jam* (*tj*) protein (Fig. 2C), a transcription factor detected in nuclei of cyst progenitors and early somatic cyst cells in wild-type (Fig. 2B). The number of Tj-positive somatic cyst cell nuclei detected in *stet* mutant testes varied, ranging from 20 to 90, compared with 70 to 80 Tj-positive somatic cyst cell nuclei detected in wild-type testes. Somatic cyst cells were also detected in *stet* mutant testes by several nuclear targeted *lacZ* enhancer-trap markers (11, 600, 473, data not shown).

stet is required for encapsulation of male germ cells by somatic cyst cells

Despite the presence of somatic cyst cell nuclei, cyst cells did not appear to envelop germ cells in *stet* mutant testes. In wild type, somatic cyst progenitors and cyst cells surround early germ cells in a net-like pattern that can be visualized using cytoplasmic cyst cell markers. In wild-type testes, β-galactosidase activity encoded by the 17-en-40 insert (*wingless-lacZ* enhancer trap marker) was detectable throughout the cell body and cytoplasmic extensions of somatic cyst cells as they surround the developing germ cells (Fig. 2D, arrows). In *stet* mutant testes stained for the same cytoplasmic cyst cell marker, cyst cells appeared round (Fig. 2E, arrows), with a small percent (10-30%) having detectable short cytoplasmic extensions (Fig. 2E, arrowheads). Similar results were obtained by expressing a cytoplasmic UAS-GFP under the control of the *patched*-GAL4 (*ptc*-GAL4) transcriptional activator. In wild-type testes, the GFP-positive cytoplasm of somatic cyst cells formed a net-like pattern surrounding the germ cells (Fig. 2F, arrows). In contrast, in *stet* mutant testes cyst cells were mostly detected as round GFP-positive structures (Fig. 2G, arrows), and only a few GFP-positive cytoplasmic extensions were observed (Fig. 2G, arrowheads). The number of somatic cyst cells in *stet* mutant testes detected with cytoplasmic markers (ranging from seven to 46) was lower than the number of cyst cells (20 to 90) detected with the nuclear marker Tj.

Analysis of male germline clones indicated that *stet* function is required in germ cells. Clones of cells that lack the *stet* gene were generated in *stet*/+ animals using a FRT/FLP recombination system (Xu and Rubin, 1993) and identified by lack of expression of a nuclear targeted GFP (see Materials and Methods). GFP is expressed under control of the ubiquitin promotor, allowing for detection of both, the round nuclei of germ cells (Fig. 3A, arrowheads) and the triangular shaped nuclei of somatic cells (Fig. 3A, arrows). Control clones wild-type for *stet* produced clusters of GFP-negative germ cells (Fig. 3B, circles) that developed normally into spermatocytes, based on appearance by phase contrast microscopy (data not shown) and nuclear size when stained with DAPI (Fig. 3C). In contrast, *stet/stet* mutant germ cells did not differentiate into spermatocytes. Instead, germline clones produced large

Fig. 5. Early germ cells accumulate in *stet* mutant germaria. (A) Diagram of a wild-type germarium. Germ cells in dark gray, somatic cells in light gray. Note spectrosomes (sp) in germline stem cells (gsc) and cystoblasts (cb) in region 1, and branched fusomes (fu) in cystocytes (cys). In region 1 and 2A, germ cells are surrounded by cytoplasmic extensions (light gray) from inner sheath cells (isc). In region 2B, germ cells become enclosed by somatic follicle cells (fc). Region 3 contains one egg chamber. Terminal filament cells (tfc), cap cells (cc), follicle precursor cells (fpc), as indicated. (B,H) Scale bars: 5 μm. (B-G) Germaria from (B,D,F) wild-type and (C,E,G) *stet* mutant females; apical tips towards the left. (B,C) Immunofluorescense staining with anti-Sxl. (B) Wild type: stem cells and cystoblasts at the tip have high level of cytoplasmic Sxl (arrow). (C) *stet*: many early germ cells with high level of cytoplasmic Sxl (arrows). (D,E) Immunofluorescense staining with anti-α-spectrin. (D) Wild-type: α-spectrin in spectrosome (arrows) in stem cells and cystoblasts and the branching fusome (arrowhead) in cystocytes. (E) *stet*: many cells with spectrosomes (arrows). (F,G) Expression of UAS-GFP under control of the *en*-GAL4 activator in inner sheath cells in region 1 and 2A. (F) Wild type: extensions from inner sheath cells extend among germ cells in region 1 and 2A (arrows). (G) *stet*: inner sheath cells are present and express GFP (arrows), but no cytoplasmic extensions were detected. (H) Electron microscope image showing a cytoplasmic extension (arrowheads) originating from an inner sheath cell (n, nucleus of inner sheath cell) and extending between a germline stem cell (s) and a cystoblast (c). Cap cell (cc), spectrosome (sp), as indicated. The image was taken by A. T. Carpenter from the wild-type germarium analyzed by Carpenter (Carpenter, 1975).

clusters of GFP-negative cells (Fig. 3D, circle, Fig. 3F) resembling early germ cells, based on appearance by phase contrast microscopy (data not shown) and by their small, bright nuclei when stained with DAPI (Fig. 3E). The cells in *stet* mutant clones expressed *piwi* mRNA (Fig. 3G, arrowheads) and other early germ cell markers normally restricted to the anterior tip of the testis. Staining with *esg* mRNA and α-spectrin (data not shown) revealed that the cells within individual *stet* mutant clones were a mixed population resembling stem cells, gonialblasts and spermatogonia, much as the germ cells accumulating in testes from *stet* homozygous mutant males.

Loss of *stet* function in the germline affected association with the *stet*/+ heterozygous somatic cyst cells. Based on GFP-expression, 60% (100 clones tested) of *stet* mutant germ line clones were not associated with triangular GFP-positive nuclei (Fig. 3F). Triangular GFP-positive nuclei were detected on top,

under or at the side of the clusters of *stet* mutant germ cells in the remaining 40% of the clones. In 30% we detected 1 GFP-positive nucleus. In 10% we detected two GFP-positive nuclei (data not shown). The triangular GFP-positive somatic cyst cell nuclei could have been associated with the *stet* mutant germ cell clone or with a neighboring *stet*/+ germ cell cluster. The presence of somatic cyst cells associated with *stet* mutant germ cell clones was further examined by anti-Tj staining. The nuclear early cyst cell nuclei marker Tj was detected in somatic cyst cell nuclei at the apical tip of wild-type testes, but not in later stage cyst cells. In testes containing *stet* mutant germ cells clones, many Tj-positive cyst cells were detected at the apical testes tip (Fig. 3H, arrows). However, nuclei expressing the early cyst cell marker Tj were usually not found associated with the cluster of *stet* mutant germ cells. For 21 out of 25 *stet* mutant germ cell clones carefully examined in all planes of focus, we did not detect any Tj-positive nuclei in, on top of, under or next to the clone (Fig. 3I). For three of the 25 *stet* mutant germ cell clones, we observed one associated Tj-positive nucleus (Fig. 3J, arrow). For one out of the 25 *stet* mutant germ cell clones, we observed two associated Tj-

Table 1. Lesions in *stet* alleles

Allele	Base pair change*	Amino acid change
stet[2]	G(857)A	W (286) STOP
stet[z3-3671]	T(680)A	Y (227) STOP
stet[8A, 3]	A(489)T	S (164) C (PM)
stet[z3-0369]	C(768)T	H (257) T (PM)
stet[z3-3835, z3-4806]	G(879)A	A(294)T
stet[871]	TTC(641)TTCGGTGAA	FV (214) FVSVSTOP

*Base pair 1 was assigned as the A in the AUG for the predicted start codon in the testes cDNA
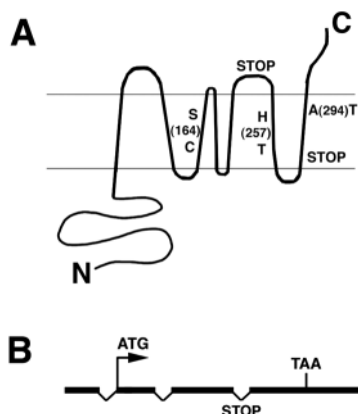
PM, conserved protease motif.

Fig. 6. *stet* encodes a predicted transmembrane protein homolog of *rho*. (A) Predicted structure of the *stet* transmembrane protein, showing seven transmembrane domains, placing the N terminus and the C terminus on opposite sites of the membrane (TMpred, ExPASy Molecular Biology Server). Amino acid substitutes in sequenced *stet* alleles (Table 1) are indicated. (B) Intron-exon structure based on the sequence of the testis cDNA, with predicted start codon in exon 2, stop codon in exon 4, and indicating the splice site mutation between exon 3 and 4 in *stet* [871] leading to a premature stop codon.

positive nuclei (Fig. 3K, arrows). None of the 25 *stet* mutant germ cell clones was associated with more than two Tj-positive nuclei.

To test whether somatic cyst cells associated with *stet* mutant germ cell clones instead expressed late cyst cell markers, we stained for the late cyst cell marker *eyes absent* (*eya*). Eya is normally expressed in nuclei of cyst cells associated with spermatogonia. For 50 *stet* mutant clones examined, we did not detect any Eya-positive cyst cell nuclei on top, within or under the clone. Eya-positive cyst cell nuclei were detected next to the *stet* mutant germ cell clones (Fig. 3L, arrows). However, these cyst cells could have been associated either with the *stet* mutant clone or with a neighboring cluster of *stet*/+ spermatocytes.

Together our analysis indicates that most *stet* mutant germ cell clones were not associated with the two accompanying somatic cyst cells.

stet mutations cause defects in female germ cell differentiation

Females mutant for loss-of-function *stet* alleles that cause severe defects in male germ cell differentiation produced few progeny (one to three adult progeny/female) and showed a variety of defects in oogenesis. In young *stet* mutant females, 60% of the ovarioles contained egg chambers at several different stages of differentiation (Fig. 4B). DAPI staining (Fig. 4C) and phase contrast microscopy (data not shown) revealed that egg chambers from *stet* mutant females often contained abnormal numbers and arrangements of germ cells. In older *stet* mutant females, 90% of the ovarioles usually had only a few egg chambers, which commonly showed signs of degeneration (Fig. 4D). By 2 weeks after hatching, all ovarioles from *stet* mutant females were mostly empty, except for the germaria, which contained increased numbers of early germ cells as described below. *stet* mutant females became completely sterile with increasing age.

Early germ cells accumulate in the germarium in *stet* mutant females

Early germ cells appeared to accumulate at the apical tip of the germarium in both young and old *stet* mutant females. In wild-type germaria, germline stem cells lie at the tip, followed by their immediate daughters, the cystoblasts, and then the interconnected cystocytes (Fig. 5A). In wild type, germline stem cells and cystoblasts can be distinguished from later stage germ cells by several subcellular markers. *Sex-lethal* (*Sxl*) protein accumulates in the cytoplasm of stem cells and cystoblasts to a much higher level than in later stage germ cells (Fig. 5B, arrow) (Bopp et al., 1993). In addition, α-spectrin is localized to the ball-shaped spectrosome in wild-type stem cells and cystoblasts (Fig. 5D, arrows) but localizes to the branched fusome in cystocytes (Fig. 5D, arrowhead). Germaria from *stet* mutant females had an elevated number (ranging from the normal six to 75 cells) of early germ cells with cytoplasmic Sxl (Fig. 5C, arrows) and a spectrosome (Fig. 5E, arrows) compared with wild-type germaria (four to six cells). The apparent accumulation of cells resembling stem cells and/or cystoblasts in *stet* mutant germaria suggests that wild-type function of *stet* in females plays a role in allowing differentiation of early germ cells.

stet is required for enclosure of female germ cells by cytoplasmic extensions from inner sheath cells

Wild-type function of *stet* appears to facilitate the contacts between female germ cells and a population of somatic cells in region 1 and 2A of the germarium. In wild-type and *stet* mutant germaria, 11 to 12 inner sheath cells were detected in region 1 and 2A of the germarium based on the nuclear targeted *lacZ* enhancer trap marker I-72 for inner sheath cells (data not shown). These inner sheath cells form cytoplasmic extensions between stem cells, cystoblasts and clusters of cystocytes in region 1 and 2A of the germarium, that can be seen at the ultrastructural level (Fig. 5H, arrows). The cytoplasmic extensions can also be seen upon expression of cytoplasmic GFP (UAS-GFP) under control of either an *engrailed*-GAL4 (*en*-GAL4, Fig. 5F) or a *ptc*-GAL4 transcriptional activator (data not shown). In wild-type germaria, we detected nine to 12 GFP-positive extensions from inner sheath cells between germ cells in region 1 and 2A of the germarium. In germaria from *stet* mutant females, six to 12 GFP-positive inner sheath cells were present (Fig. 5G, arrows). However, they did not form normal numbers of cytoplasmic extensions. In 50% of the germaria from newly enclosed females, two to eight GFP-positive cytoplasmic extensions from inner sheath cells were detected around or between germ cells. By 1 week after hatching, no cytoplasmic extensions from inner sheath cells were detected in germaria from *stet* mutant females.

The *stet* mutant phenotype is caused by mutations in a *rho* homolog

To explore the mechanism of action of *stet*, we identified the *stet* gene product by positional cloning. We localized the *stet* gene to cytological region 62A1 by recombination analysis and deficiency complementation. The *stet* mutation was uncovered by *Df(3L)PX62*, which removes ~60 kb of genomic DNA in 62A1. Analysis of the genome sequence in this region revealed 12 potential transcription units (data not shown, see Materials and Methods).
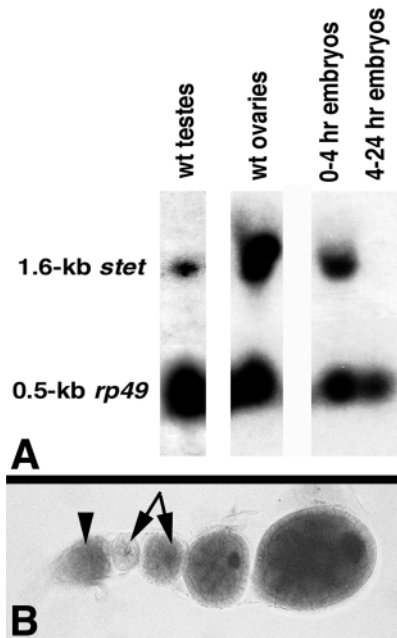
Fig. 7. *stet* is expressed in testes and ovaries. (A) Northern blot showing *stet* transcript in testes, ovaries and early embryos and *rp49* loading control in all lanes. Testes lane, 5 μg poly(A)$^+$ RNA loaded; ovary and embryo lanes, 1 μg poly(A)$^+$ RNA loaded. (B) Wild-type ovariole hybridized in situ with *stet* mRNA. Note expression in the germarium (arrowhead) and localization of the transcript to the oocyte in egg chambers (arrows).

Sequence analysis of genomic DNA from several EMS induced *stet* alleles identified *stet* as a predicted seven transmembrane protein (Table 1, Fig. 6A). The predicted *stet* protein showed high sequence similarity to the *Drosophila rho* protein (data not shown) and had been published under the names CT5484 (FlyBase, 1999), *rhomboid-2* (*rho-2*) (Wasserman et al., 2000) and *brother of rhomboid* (*brho*) (Guichard et al., 2000). In the following, we will refer to the *stet* gene product as *stet* based on naming genes by the mutant phenotype. Two strong *stet* alleles introduced stop codons in the *stet* protein-coding region, truncating the predicted protein (Fig. 6A). Another strong *stet* allele introduced a splice site change resulting in a frame shift that led to a premature stop codon in the predicted *stet* protein (Fig. 6B). Several other EMS alleles altered conserved amino acids in the predicted *stet* transmembrane domains (Fig. 6A); *stet* ^{8A}, *stet* ^{3} and *stet* $^{z3–0369}$ had amino acid replacements in the conserved protease motif. Comparison of the genomic sequence with several independent cDNAs isolated from a testes cDNA library revealed that the *stet* testis transcript contained four exons (Fig. 6B). The predicted protein from the *stet* testes cDNA had stop codons in all three reading frames upstream of the predicted initial methionine, located in exon 2.

We detected *stet* transcript on northern blots from adult testes, adult ovaries and 0-4 hour embryos. Transcript was not detected on similarly loaded northern blots of mRNA from 4-24 hour embryos (Fig. 7A). Although the *stet* mutant phenotype clearly demonstrates a requirement for *stet* function in male germ cells, we did not detected *stet* mRNA by in situ hybridization or *stet* protein by immunofluorescence staining
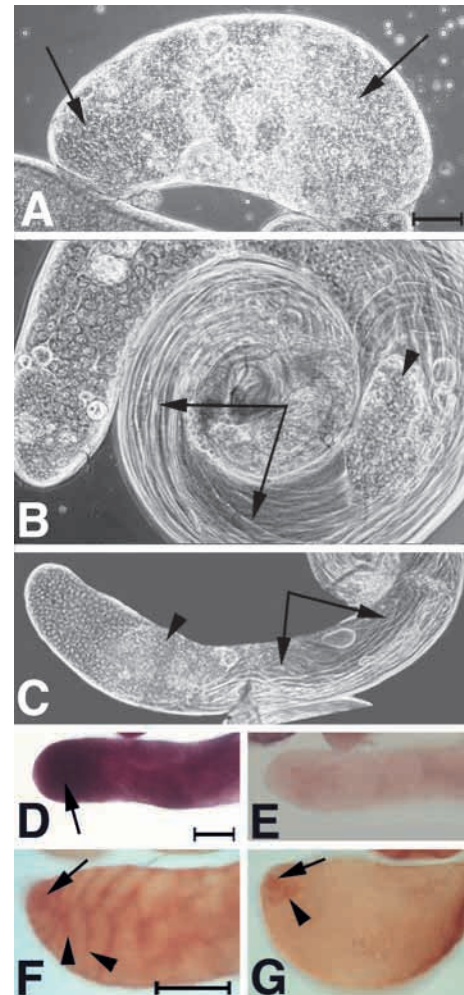
Fig. 8. *stet* may function through *Egfr* signaling. (A-C) Phase contrast images. (A) *stet* mutant testis filled with small cells (arrows). (B,C) Spermatogenesis is restored in *stet* mutant testes expressing (B) a UAS-*stet* construct and (C) a UAS-*rho* construct in germ cells, note elongated sperm bundles (arrows). Occasionally, clusters of *stet* mutant germ cells can still be observed (arrowheads). (D,E) In situ hybridization to adult wild-type testes. (D) *Star* mRNA at high levels in germ cells at the apical tip (arrow). (E) Sense-control: no staining. (F,G) Immunocytochemical stain with anti-activated MAP-kinase (DP-ERK) to adult testes. (F) Wild-type: activated MAP-kinase in the somatic hub cells (arrow) and in the cytoplasm of cyst cells (arrowheads). (G) *stet*: activated MAP-kinase in somatic hub cells (arrow) and a few cyst cells (arrowhead) next to the hub. Scale bars: in A, 0.1 mm for A-C; in D, 0.1 mm for D,E; in F, 0.1 mm for F,G.

of whole testes. The high load required to detect *stet* transcript on northern blot and the failure to detect *stet* RNA or protein in whole mount testes suggest that *stet* is expressed at extremely low level. Similarly, although *stet* function is clearly required in region 1 and 2A of the germarium, neither *stet* mRNA nor *stet* protein accumulated at detectable levels at the tip of the germarium. *stet* mRNA was detected in germ cells in region 2B and 3 of the germarium (Fig. 7B, arrowhead). Signal from the *stet* mRNA was extremely low in germ cells of stage 1 and 2 egg chambers, but increased in germ cells of stage 3 to stage 8 egg chambers. In stage 1 to 8 egg chambers,

stet mRNA appeared to accumulate in the posterior region of the egg chambers, in the position of the developing oocyte (Fig. 7B, arrows).

stet may play a role in *Egfr* signaling

The identity of *stet* was confirmed by rescue experiments. Consistent with *stet* function in germ cells, expression of a UAS-*stet*-cDNA in germ cells of *stet* mutant testes under control of the germ cell-specific driver *nanos*-GAL4-VP16 restored spermatogenesis (Fig. 8B). As expression with the UAS-GAL4 system is temperature dependent, rescue was not always complete and occasionally clusters of *stet* mutant germ cells were detected in the testes (Fig. 8B, arrowhead). In contrast, expression of UAS-*stet* under control of the somatic cell driver *ptc*-GAL4 did not rescue the *stet* mutant phenotype (data not shown), suggesting that *stet* function in germ cells is both required and sufficient to allow germ cell differentiation.

Expression of *rho* in germ cells of *stet* mutant testes also restored spermatogenesis (Fig. 8C), indicating that *stet* and *rho* may function through the same biochemical mechanism. To explore how *stet* function in early male germ cells might relate to the *Egfr* signal transduction pathway, we tested the expression and effects of other components of the pathway on early male germ cell differentiation. Expression of secreted forms of the *Egfr* ligands *spi* and *grk* in male germ cells under the control of the *nos*-GAL4 activator did not modify the *stet* mutant phenotype (data not shown), raising the possibility that another ligand may play a role in male germ cells. *rho* normally acts synergistically with the transmembrane protein *Star* within the signaling cell to activate *spi* (Rutledge et al., 1992; Kolodkin et al., 1994; Pickup and Banerjee, 1999; Guichard et al., 1999). In situ hybridization with a *Star* mRNA probe to wild-type testes revealed high levels of *Star* expression at the apical tip (Fig. 8D, arrow).

Consistent with a potential role for the *Egfr* in somatic cells, activated MAP-kinase is detectable in somatic cyst cells of wild-type testes (Fig. 8F, arrowheads) (Kiger et al., 2000). In *stet* mutant testes, MAP-kinase expression was restricted to the somatic hub cells (Fig. 8G, arrow) and a few (two to five) cells next to the somatic hub in the position corresponding to that of cyst progenitor cells (Fig. 8F, arrowhead). Although cyst cells were present in *stet* mutant testes (Fig. 2C), we did not detect activated MAP-kinase in cyst cells displaced away from the hub. Likewise, we detected activated MAP-kinase in the cytoplasmic extensions of inner sheath cells of wild-type germaria, but only in a few inner sheath cells in germaria from *stet* mutant females (data not shown).

DISCUSSION

The *stet* gene plays a crucial role in germ cell differentiation in both males and females. In animals that lack *stet* function, somatic support cells failed to surround germ cells properly and germ cells accumulated at early stages of differentiation. Mosaic analysis in testes suggested that *stet* function is required in germ cells for normal association between early germ cells and somatic cyst cells. This, along with the molecular identity of the *stet* gene, suggests that *stet* activates signaling from germ cells to the soma to allow normal interactions between germ cells and somatic support cells.

The *stet* gene encodes a homolog of *rho*, which plays an essential role in *Egfr* signaling (Sturtevant et al., 1993; Sapir et al., 1998; Wassermann and Freeman, 1998). Rho has recently been shown to localize to the Golgi apparatus, where it acts as a protease to cleave the *Egfr* ligand *spi* (Lee et al., 2001; Urban et al., 2001). The *stet* protein also localized to the Golgi apparatus in cell culture experiments (Ghiglione et al., 2002), and contains the protease motif described for Rho (Urban et al., 2001). Consistent with the idea that *stet* may encode a protease, three strong *stet* alleles alter residues in the conserved protease domain.

Mosaic analysis and rescue experiments showed that *stet* function is required in male germ cells for normal germ cell differentiation. We cannot exclude the possibility that this is a cell-autonomous function of *stet* within the germ cells. However, the *rho* family of proteins have been shown to play roles in the production of signals sent to neighboring cells, and do not seem to be directly required for differentiation of the ligand producing cell itself (Golembo et al., 1996; Wasserman et al., 2000). We therefore favor the idea that *stet* functions primarily by activating signaling from germ cells to somatic cells. We propose that once proper contacts between germ cells and somatic cells are established, signals from somatic cells then regulate germ cell differentiation. We hypothesize that germ cells in *stet* mutants fail to differentiate because they lack the somatic micro-environment that provides essential cues regulating germ cell differentiation.

Experiments in wing discs demonstrate that *stet* is able to collaborate with *Star* to promote signaling through the *Egfr*/MAP-kinase pathway. *stet* can activate the *Egfr* ligands *spi* and *grk* when ectopically expressed in wing discs or follicle cells (Guichard et al., 2000; Ghiglione et al., 2002). In this study, we showed that expression of *rho* in germ cells can substitute for *stet* function, and that *Star* is expressed at the tip of wild-type testes. In addition, in *stet* mutant testes most somatic cyst cells failed to express activated MAP-kinase, the downstream indicator for *Egfr* signaling. Based on these observations, we propose that the *stet* gene functions as an activator of signaling from early germ cells to the *Egfr* presented on the surface of somatic cells and that activation of the *Egfr* in somatic cells is required to establish normal interactions between germ cells and somatic cells.

Testes from animals carrying a temperature-sensitive allele of the *Egfr* showed accumulation of germ cells that appeared to be stem cells, gonialblasts and spermatogonia (Kiger et al., 2000). This similarity to the *stet* mutant phenotype in testes is consistent with *stet* and the *Egfr* functioning in the same pathway. However, the *Egfr*^{ts} mutant phenotype in testes did not exactly resemble the *stet* mutant phenotype. In *stet* mutant testes, somatic cyst cells did not envelope clusters of early germ cells properly. Testes from *Egfr*^{ts} mutant animals displayed many defects in the association of somatic cyst cells and early germ cells, including some cases in which germ cell clusters were associated with multiple somatic cyst cells (Kiger et al., 2000). As analysis of the *Egfr*^{ts} phenotype was performed after a temperature shift, we hypothesize that testes from *Egfr*^{ts} animals may have had sufficient residual *Egfr* activity to allow some and possibly abnormal association of early germ cells and somatic cyst cells. In addition, the *Egfr*^{ts} mutant may not be null for *Egfr* function at 29°C, the temperature assayed. Consistent with this likely possibility,

Kiger et al. (Kiger et al., 2000) have reported a failure to recover cyst cell clones mutant for *Egfr* null alleles, even though they did detect somatic cyst cells in the *Egfr*[ts] allele. In contrast, in our study we report the phenotype of animals null mutant for *stet* throughout development.

stet may activate a yet unidentified *Egfr* ligand to recruit somatic cells for germ cell encapsulation. Even though *stet* can activate *spi* and *grk* when ectopically co-expressed in wing discs (Guichard et al., 2000), expression of secreted forms of *spi* or *grk* in male germ cells did not rescue the *stet* mutant phenotype in our study. Loss-of-function alleles of *grk* that cause severe defects in female gametogenesis did not show an early germ cell over-proliferation phenotype in testes (C. S., unpublished), suggesting that *stet* does not function through *grk* activation. In females, eggs laid by *stet* mutant mothers did not display the *grk* or *spi* mutant phenotypes, but instead either showed a variety of defects or developed into phenotypically normal adults. Further investigation of the *Egfr* signal transduction pathway remains to be undertaken to identify additional components of the pathway and test their potential role in interactions between early germ cells and surrounding somatic cells.

The early stages of gametogenesis in *Drosophila* are strikingly similar in males and females in that, in both sexes, germ cells are in constant contact with encapsulating somatic cells. Based on ultrastructural studies by electron microscopy and light microscopy analysis using several markers (Margolis and Spradling, 1995) (this study), the inner sheath cells in region 1 and 2A of the germarium appear to form cytoplasmic extensions that contact female germ line stem cells, cystoblasts and cystocytes. Our study provides the first insight into the function of the inner sheath cells. In *stet* mutant females, the cytoplasmic extensions from the inner sheath cells failed to surround the germ cells and the germ cells failed to progress to the cystocyte stages. We propose that the inner sheath cells at the tip of the germarium may play a role similar to the somatic cyst cells surrounding germ cells in testes, providing a microenvironment that directs female germ cell differentiation.

Our data predict a new function for the *Egfr* signaling pathway in the female gonad. *Egfr* signaling, activated by *stet*, may be required to set up the normal interactions of early female germ cells and somatic inner sheath cells in region 1 and 2A of the germarium. We did not observe accumulation of early germ cells with cytoplasmic *Sxl* protein and spectrosomes at the tip of the germarium after shifting animals carrying the *Egfr*[ts] allele to the restrictive temperature as adults (data not shown). However, many ovarioles from females carrying *Egfr*[ts] alleles also did not display defects at later stages of oogenesis in these experiments, again indicating that the *Egfr*[ts] allele had residual *Egfr* activity and may not reflect the *Egfr* loss-of-function situation.

We cannot rule out the possibility that *stet* activates other signaling pathways to set up proper physical interactions between germ cells and somatic support cells. In females, normal encapsulation of germ cells by somatic follicle cells requires the neurogenic genes *brainiac* (*brn*) and *egghead* (*egh*). *brn* encodes a secreted protein (Goode et al., 1996a) and *egh* encodes a secreted or transmembrane protein (Goode et al., 1996b). Double mutant combinations of *grk* and *brn* displayed much stronger defects in encapsulation of germ cells than either *grk* or *brn* mutants alone, suggesting that the *brn* and *egh* pathway and the *Egfr* pathway function partially redundantly in formation of the prefollicular epithelium (Goode et al., 1992). This opens the possibility that encapsulation of early female germ cells by inner sheath cells and encapsulation of male germ cells by somatic cyst cells depend on another signaling pathway instead of, or in addition to the *Egfr* signal transduction pathway.

REFERENCES

Ashburner, M. (1989). Drosophila. *A Laboratory Manual*. New York: Cold Spring Harbor Laboratory Press.

Berry, L. W., Westlund, B. and Schedl, T. (1997). Germ-line tumor formation caused by activation of *glp-1*, a *Caenorhabditis elegans* member of the *Notch* family of receptors. *Development* **124**, 925-936.

Bier, E., Jan, L. Y. and Jan, Y. N. (1990). *rhomboid*, a gene required for dorsoventral axis establishment and peripheral nervous system development in *Drosophila melanogaster*. *Genes Dev.* **3**, 190-203.

Bitgood, M. J., Shen, L. and McMahon, A. P. (1996). Sertoli cell signaling by Desert hedgehog regulates the male germline. *Curr. Biol.* **6**, 298-304.

Bopp, D., Horabin, J. I., Lersch, R. A., Cline, T. W. and Schedl, P. (1993). Expression of the *Sex-lethal* gene is controlled at multiple levels during *Drosophila* oogenesis. *Development* **118**, 797-812.

Bünning, J. (1994). *The Insect Ovary*. London: Chapman and Hall.

Carpenter, A. T. (1975). Electron microscopy of meiosis in *Drosophila melanogaster* females. I. Structure, arrangement, and temporal change of the synaptonemal complex in wild-type. *Chromosoma* **51**, 157-182.

Church, D. L., Guan, K. L. and Lambie, E. J. (1995). Three genes of the Map kinase cascade, *mek-2, mpk-1/sur-1 and let-60 ras*, are required for meiotic cell cycle progression in *Caenorhabditis elegans*. *Development* **121**, 2525-2535.

Desjardins, C. and Ewing, L. L. (1993). *Cell and Molecular Biology of the Testis*. New York: Oxford University Press.

Erickson, G. F. (1986). An analysis of follicle development and ovum maturation. *Semin. Reprod. Endocrinol*. **4**, 233-254.

FlyBase (1999). The FlyBase database of the *Drosophila* genome projects and community literature. *Nucleic Acids Res.* **27**, 85-88.

Freeman, M. (1998). Complexity of the EGF receptor signaling revealed in *Drosophila. Curr. Opin. Genet. Dev.* **8**, 407-411.

Ghiglione, C., Bach, E. A., Paraiso, Y., Carraway, K L., III, Noselli, S. and Perrimon, N. (2002). Mechanism of activation of the *Drosophila* EGF receptor by the TGFα ligand Gurken during oogenesis. *Development* **129**, 175-186.

Gönczy, P., Viswanathan, S. and DiNardo, S. (1992). Probing

spermatogenesis in *Drosophila* with P-element enhancer detectors. *Development* **114**, 89-98.

Gönczy, P. and DiNardo, S. (1996). The germ line regulates somatic cyst cell proliferation and fate during *Drosophila* spermatogenesis. *Development* **122**, 2437-2447.

Gönczy, P., Matunis, E. and DiNardo, S. (1997). *bag-of-marbles* and *benign gonial cell neoplasm* act in the germline to restrict proliferation during *Drosophila* spermatogenesis. *Development* **124**, 4361-4371.

Golembo, M., Raz, E. and Shilo, B.-Z. (1996). The *Drosophila* embryonic midline is the site of Spitz processing, and induces activation of the EGF receptor in the ventral ectoderm. *Development* **122**, 3363-3370.

Gonzales-Reyes, A., Elliott, H. and St Johnston, D. (1995). Polarization of both major body axes in *Drosophila* by *gurken-torpedo* signaling. *Nature* **375**, 654-658.

Goode, S., Wright, D. and Mahowald, A. P. (1992). The neurogenic locus *brainiac* cooperates with the *Drosophila* EGF receptor to establish the ovarian follicle and to determine its dorsal-ventral polarity. *Development* **116**, 177-192.

Goode, S., Morgan, M., Liang, Y.-P. and Mahowald, A. P. (1996a). *brainiac* encodes a novel, putative secreted protein that cooperates with *grk* TGFα in the genesis of the follicular epithelium. *Dev. Biol.* **178**, 35-50.

Goode, S., Melnick, M., Chou, T.-B. and Perrimon, N. (1996b). The neurogenic genes *egghead* and *brainiac* define a novel signaling pathway essential for epithelial morphogenesis during *Drosophila* oogenesis. *Development* **122**, 3863-3879.

Guichard, A., Biehs, B., Sturtevant, M. A., Wickline, L., Chacko, J., Howard, K. and Bier, E. (1999). *rhomboid* and *Star* interact synergistically to promote EGFR/MAPK signaling during *Drosophila* wing vein development. *Development* **126**, 2663-2676.

Guichard, A., Roark, M., Ronshaugen, M. and Bier, E. (2000). *brother of rhomboid*, a rhomboid-related gene expressed during early *Drosophila* oogenesis, promotes EGF-R/MAPK signaling. *Dev. Biol.* **226**, 255-266.

Hall, D. H., Winfrey, V. P., Blaeuer, G., Hoffman, L. H., Furuta, T., Rose, K. L., Hobert, O. and Greenstein, D. (1999). Ultrastructural features of the adult hermaphrodite gonad of *Caenorhabditis elegans*: relations between germ line and soma. *Dev. Biol.* **212**, 101-123.

Hardy, R. W., Tokuyasu, K. T., Lindsley, D. L. and Garavito, M. (1979). The germinal proliferation center in the testis of *Drosophila melanogaster*. *J. Ultrastruct. Res.* **69**, 180-190.

Hime, G. R., Brill, J. A. and Fuller, M. T. (1996). Assembly of ring canals in the male germ line from structural components of the contractile ring. *J. Cell Sci.* **109**, 2779-2788.

Hsueh, A. J. and Schomberg, D. W. (1993). *Ovarian Cell Interactions*. Berlin: Springer Verlag.

Kammermeyer, K. L. and Wadsworth, S. C. (1987). Expression of *Drosophila* epidermal growth factor homologue in mitotic cell populations. *Development* **100**, 201-210.

Kiger, A. A., White-Cooper, H. and Fuller, M. T. (2000). Somatic support cells restrict germline stem cell self-renewal and promote differentiation. *Nature* **407**, 750-754.

Kiger, A. A. and Fuller, M. T. (2001). Male germ-line stem cells. In *Stem Cell Biology* (ed. D. R. Marshak, R. L. Gardner and D. Gottlieb), pp. 149-187. New York: Cold Spring Harbor Laboratory Press.

Kimble, J. and White, J. (1981). On the control of germ cell development in *Caenorhabditis elegans*. *Dev. Biol.* **81**, 208-219.

King, R. C. (1970). *Ovarian Development in* Drosophila melanogaster. New York, London: Academic Press.

King, F. J. and Lin, H. (1999). Somatic signaling mediated by the *fs(1)Yb* is essential for germline stem cell maintenance during *Drosophila* oogenesis. *Development* **126**, 1833-1844.

Klingler, M. and Gergen, J. P. (1993). Regulation of *runt* transcription by *Drosophila* segmentation genes. *Mech. Dev.* **43**, 3-19.

Kolodkin, A. L., Pickup, A. T., Lin, D. M., Goodman, C. S. and Banerjee, U. (1994). Characterization of *Star* and its interactions with *sevenless* and EGF receptor during photoreceptor cell development in *Drosophila*. *Development* **120**, 1731-1745.

Lee, J. R., Urban, S., Garvey, C. F. and Freeman, M. (2001). Regulated intracellular ligand transport and proteolysis control EGF signal activation in *Drosophila*. *Cell* **107**, 161-171.

Lev, Z., Shilo, B.-Z. and Kimchie, Z. (1985). Developmental changes in the expression of the *Drosophila melanogaster* epidermal growth factor receptor gene. *Dev. Biol.* **110**, 499-502.

Lindsley, D. L. and Zimm, G. G. (1992). *The Genome of* Drosophila melanogaster. San Diego: Academic Press.

Matunis, E., Tran, J., Gönczy, P. and DiNardo, S. (1997). *punt* and *schnurri* regulate a somatically derived signal that restricts proliferation of committed progenitors in the germline. *Development* **124**, 4383-4391.

Margolis, J. and Spradling, A. C. (1995). Identification and behavior of epithelial stem cells in the *Drosophila* ovary. *Development* **121**, 3797-3807.

Marziali, G., Lazzaro, D. and Sorrentino, V. (1993). Binding of germ cells to mutant Sl^d Sertoli cells is defective and is rescued by expression of the transmembrane form of the *c-kit* ligand. *Dev. Biol.* **157**, 182-190.

Matzug, M. M. (2000). Revelations of ovarian follicle biology from gene knockout mice. *Mol. Cell. Endocrinol.* **163**, 61-66.

McCarter, J., Bartlett, B., Dang, T. and Schedl, T. (1997). Soma-germ cell interactions in *Caenorhabditis elegans*: Multiple events of hermaphrodite germline development require the somatic sheath and spermathecal lineage. *Dev. Biol.* **181**, 121-143.

Morgan, M. M. and Mahowald, A. P. (1996). Multiple signaling pathways establish both the individuation and the polarity of the oocyte follicle in *Drosophila*. *Arch. Insect Biochem. Physiol.* **33**, 211-230.

Ojeda, S. R., Romero, C., Tapia, V. and Dissen, G. A. (2000). Neurotrophic and cell-cell dependent control of early follicular development. *Mol. Cell. Endocrinol.* **163**, 67-71.

Pesce, M., di Carlo, A. and de Felici, M. (1997). The *c-kit* receptor is involved in the adhesion of mouse primordial germ cells to somatic cells in culture. *Mech. Dev.* **68**, 37-44.

Phelps, C. B., Brand, A. H. (1998). Ectopic gene expression in *Drosophila* using GAL4 system. *Methods* **14**, 367-379.

Pickup, A. T. and Banerjee, U. (1999). The role of *Star* in the production of an activated ligand for the EGF receptor signaling pathway. *Dev. Biol.* **205**, 254-259.

Ruohola-Baker, H., Grell, E., Chou, T. B., Baker, D., Jan, L. Y., Jan, Y. N. (1993). Spatially localized *rhomboid* is required for establishment of the dorsal-ventral axis in *Drosophila* oogenesis. *Cell* **73**, 953-965.

Ray, R. P. and Schüpbach, T. (1996). Intercellular signaling and the polarization of body axes during *Drosophila* oogenesis. *Genes Dev.* **10**, 1711-1723.

Rutledge, B. J., Zhang, K., Bier, E., Jan, Y. N. and Perrimon, N. (1992). The *Drosophila spitz* gene encodes a putative EGF-like growth factor involved in dorsal-ventral axis formation and neurogenesis. *Genes Dev.* **6**, 1503-1517.

Sambrook, J., Fritsch, E. F. and Maniatis, T. (1989). *Molecular Cloning. A Laboratory Manual*. New York: Cold Spring Harbor Laboratory Press.

Sapir, A., Schweitzer, R. and Shilo, B.-Z. (1998). Sequential activation of the EGF receptor pathway during *Drosophila* oogenesis establishes the dorsoventral axis. *Development* **125**, 191-200.

Schulz, C., Perezgasga, L. and Fuller, M. T. (2002) Molecular-genetic analysis of *dPsa*, the *Drosophila* orthologue of puromycin-sensitive aminopeptidase, suggests redundancy of aminopeptidases. *Dev. Genes Evol.* **211**, 581-588.

Schüpbach, T. (1987). Germ line and soma cooperate during oogenesis to establish the dorsoventral pattern of egg shell and embryo in *Drosophila melanogaster*. *Cell* **49**, 669-707.

Schweitzer, R., Shaharabany, M., Seger, R. and Shilo, B.-Z. (1995). Secreted *spitz* triggers the DER signaling pathway and is a limiting component in embryonic ventral ectoderm determination. *Genes Dev.* **9**, 1518-1529.

Schweitzer, R. and Shilo, B.-Z. (1997). A thousand and one roles for the *Drosophila* EGF receptor. *Trends Genet.* **13**, 191-196.

Spradling, A. C (1986). P-element mediated transformation. In Drosophila*: A Practical Approach* (ed. D.B. Roberts), pp. 175-197. Oxford: IRL Press.

Sturtevant, M. A., Roark, M. and Bier, E. (1993). The *Drosophila rhomboid* gene mediates the localized formation of wing veins and interacts genetically with components of the EGF-R signaling pathway. *Genes Dev.* **7**, 961-973.

Tautz, D. and Pfeifle, C. (1989). A non-radioactive *in situ* hybridization method for the localization of specific RNAs in *Drosophila* embryos reveals translational control of the segmentation gene *hunchback*. *Chromosoma* **9B**, 81-85.

Tran, J., Brenner, T. J. and DiNardo, S. (2000). Somatic control over the germline stem cell lineage during *Drosophila* spermatogenesis. *Nature* **407**, 754-757.

Urban, S., Lee, J. R. and Freeman, M. (2001). *Drosophila* Rhomboid-1 defines a family of putative intramembrane serine proteases. *Cell* **107**, 173-182.

Wasserman, J. D. and Freeman, M. (1998). An autoregulatory cascade of EGF receptor signaling patterns the *Drosophila* egg. *Cell* **95**, 355-364.

Wasserman, J. D., Urban, S. and Freeman, M. (2000). A family of *rhomboid*-like genes: *Drosophila rhomboid-1* and *roughoid/rhomboid-3* cooperate to activate EGF receptor signaling. *Genes Dev.* **14**, 1651-1663.

Xie, T. and Spradling, A. C. (1998). *decapentaplegic* is essential for the maintenance and division of germline stem cells in the *Drosophila* ovary. *Cell* **94**, 251-260.

Xie, T. and Spradling, A. C. (2000). A niche maintaining germ line stem cells in the *Drosophila* ovary. *Science* **290**, 328-330.

Xie, T. and Spradling, A. C. (2001). The Drosophila ovary: An in vivo stem cell system. In Stem Cell Biology (ed. D. R. Marshak, R. L. Gardner and D. Gottlieb), pp. 129-148. New York: Cold Spring Harbor Laboratory Press.

Xu, T. and Rubin, G. M. (1993). Analysis of genetic mosaics in developing and adult *Drosophila* tissues. *Development* **117**, 1223-1237.